

Estimates of cyclone track predictability. I: Tropical cyclones in the Australian region

By K. FRAEDRICH* and L. M. LESLIE

Bureau of Meteorology Research Centre, Melbourne, Australia

(Received 23 February 1988; revised 2 August 1988)

SUMMARY

A nonlinear systems analysis is applied to the tracks of 249 tropical cyclones (with a six-hour sampling time) in the Australian tropics for the period 1959–1980. First estimates are obtained of the degree of their chaotic, or irregular, behaviour. The degree of chaos is estimated by normalizing all trajectories to a common initial position and measuring the average rate at which initially close pairs of pieces of trajectories diverge.

It was found from the correlation integrals calculated for the tropical cyclone tracks that the dimensionality of the underlying dynamical processes appears to be between six and eight, and that the time scale for e-folding error growth is about one day. The results of this study therefore suggest that the movement of Australian region tropical cyclones is predictable deterministically up to about 24 hours in advance. Beyond that limit, consideration must be given to statistically based techniques.

These findings were supported further by comparing the rate of growth of the observed Australian region tropical cyclone position variance with that derived from a random walk model superimposed on a mean drift. The correspondence was very close, with both the empirical and theoretical position variances growing linearly in time after approximately the first 18 to 24 hours, confirming that stochastic models have a role to play in forecasts beyond 24 hours.

1. INTRODUCTION

The forecasting of tropical cyclone tracks is a problem of great importance because of the annual loss of life and destruction of property caused by these systems. Forecasting techniques used to predict the movement of tropical cyclones vary widely, from the purely manual methods employed by operational forecasters through to the application of high resolution numerical models.

Accordingly, tropical cyclones have been identified as the major forecasting problem by all weather services affected by them, and concerted efforts have been made to forecast their movement. However, operational position forecasts still show negligible skill (McBride and Holland 1987; Iwasaki *et al.* 1987), where skill is defined as the ability to improve upon simple statistical techniques based on climatology and/or persistence (A.M.S. 1979), such as the climatology and persistence (CLIPER) models (Neumann and Pelessier 1981).

Whereas the level of skill in forecasting tropical cyclones has so far proved to be minimal, some significant variations in basic forecast difficulty have been noted. For example, the degree of accuracy required for the threshold skill level to be reached differs considerably between tropical cyclone basins around the world. In some basins the tropical cyclones follow climatological tracks much more closely than in other basins. It is of interest here to observe that the Australian–south-west Pacific basin (Fig. 1) has been identified in a study of six major tropical cyclone areas as having the highest average level of forecast difficulty (Pike and Neumann 1987).

It is clear from the discussion above that the question of the natural predictability of tropical cyclone tracks is one that needs to be resolved. The difficulty in obtaining a significant level of skill is very suggestive of the possibility that we are dealing with a highly irregular dynamical system, with very sensitive dependence on initial conditions. For predictability studies of this kind of phenomenon it is required to use appropriate methods of nonlinear systems analysis (Eckmann and Ruelle 1985; Lorenz 1985). Such

* On leave from Institut für Meteorologie, Freie Universität Berlin, F.R.G.

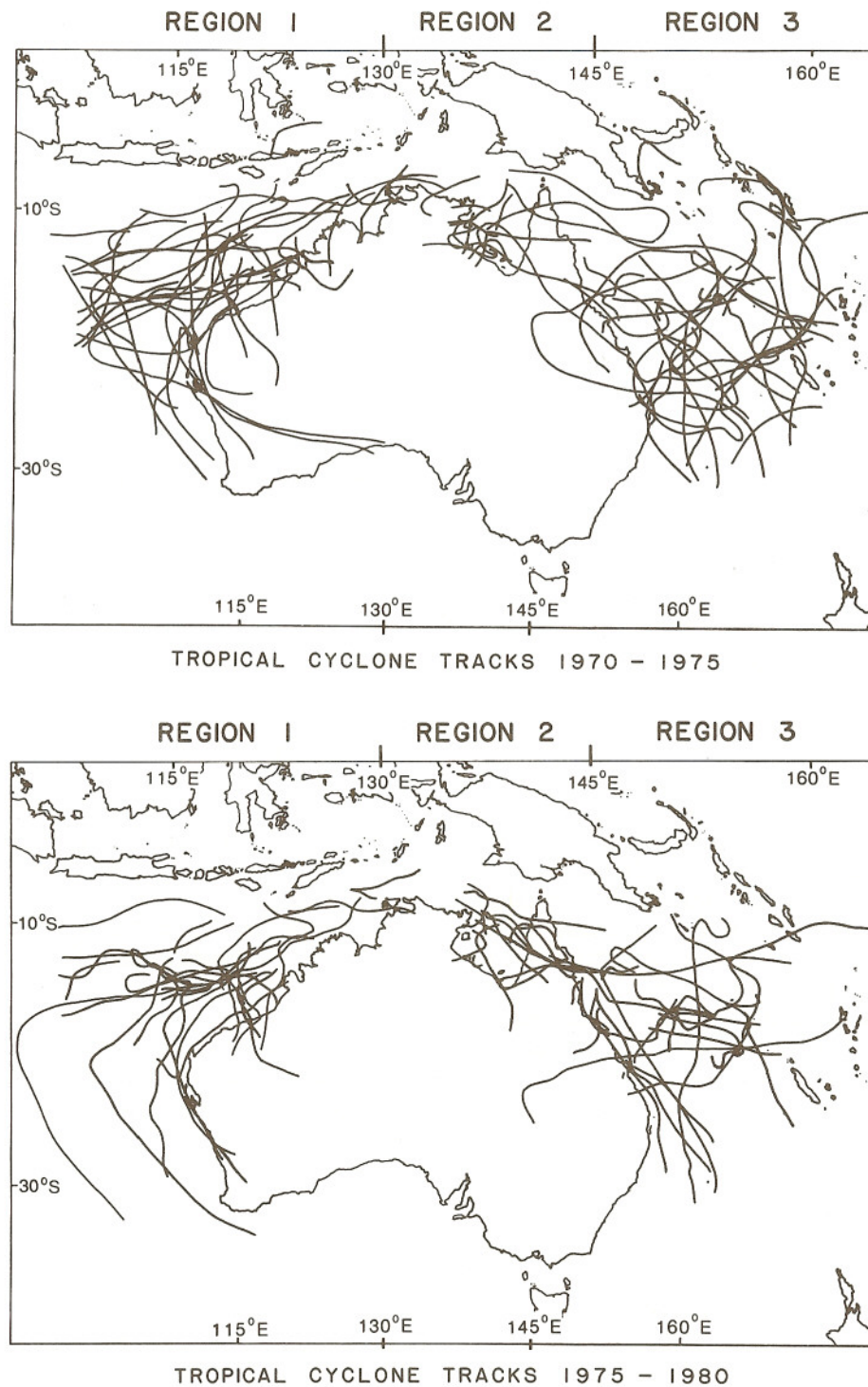


Figure 1. Two five-year samples (July 1970 to June 1975, July 1975 to June 1980) of tropical cyclone tracks in the Australian basin. Three geographical regions of cyclone origin are distinguished: Region 1 ($<130^{\circ}\text{E}$), region 2 (between 130° and 145°E), region 3 ($>145^{\circ}\text{E}$); the total basin also is considered.

techniques have been available since the early 1980s but are only just being applied to the geosciences.

In this study we will apply nonlinear systems analysis methods to the evolution of tropical cyclone tracks to estimate their predictability. This is obtained from the probability distributions obtained by counting the number of initially close and independent pairs of pieces of tropical cyclone track trajectories of successively increasing duration that lie within a prescribed distance threshold. These probability distributions can then be used to estimate both the dimensionality of the tropical cyclone attractor in phase space and the predictability time scale averaged over it.

2. PREDICTABILITY OF CYCLONE TRACKS

A relevant measure of the predictability of a dynamical system is the rate at which initially small errors grow. It can be obtained from phase space trajectories representing the time evolution of the dynamical system. From initially close trajectory pieces a suitably averaged divergence provides such a measure of predictability, because two initially close states (one being true and the other erroneous) follow different trajectories through phase space. The error growth is measured in terms of the distance between the two close states, which increases with time. In this sense the predictability of a dynamical system like the atmosphere may be related to the problem of its stability, that is, initially small differences exceeding a threshold value after a finite time span characterize an unstable process which eventually becomes unpredictable, and *vice versa*. It is obvious that different regions of the phase space may lead to different growth rates of small errors or, which is equivalent, to different rates of divergence of initially close pieces of trajectories.

As the main reason for forecast errors—at least in a perfect model—is uncertainty in the initial conditions, we estimate average bounds of predictability by the rate of separation between pairs of independent cyclones. For the analysis two simplifying assumptions are made. First, each cyclone of the pairs to be analysed starts from the same point. Relaxing this condition has shown basically unchanged results. Secondly, we have composited and analysed independent cyclone tracks originating in three distinct regions of the Australian basin (plus the total). Although this has not been proved to be the optimal discriminator, we assume that regional differentiation accounts for much of the external or climatic forcing and discard compositing with respect to the large-scale background flow because the speed and direction can change considerably during the life cycle of a cyclone.

(a) Basic concepts

(i) *Correlation integral*. A cyclone trajectory (or a part of it), $X_m(t_i)$, commencing at time t_i , is sampled in a two-dimensional space, say $X = (x, y)$, for m consecutive time steps τ :

$$X_m(t_i) = [x(t_i), y(t_i); \dots; x(t_i + (m-1)\tau), y(t_i + (m-1)\tau)]. \quad (2.1)$$

Let the distance between a pair of cyclones with independent trajectories $X_m(t_i)$, $X_m(t_j)$ (or pieces of it) be represented by the Euclidean norm after k time steps as

$$d_{ij}(k) = [\{x(t_i + k\tau) - x(t_j + k\tau)\}^2 + \{y(t_i + k\tau) - y(t_j + k\tau)\}^2]^{1/2}. \quad (2.2)$$

Then, from a total of N_m cyclone tracks all those independent pairs $N_m(l)$ are counted, whose distance is initially less than a given threshold value, say l , and remains so for the $m-1$ following time steps. That is

$$d_{ij}(k) < l, \quad k = 0, \dots, m-1. \quad (2.3)$$

This yields a probability estimate, $C_m(l)$, for independent pairs of pieces of cyclone trajectories, $X_m(t_i)$, of which $N_m(l)$ pairs remain less than a distance l apart from one another:

$$C_m(l) = N_m(l)/(N_m - 1)^2. \quad (2.4)$$

This distribution function, $C_m(l)$, is known as the correlation integral and provides quantitative measures for the underlying mathematical structure leading to irregular time evolution of the dynamical system, which occurs on attractors in phase space (Grassberger and Proccacia 1984; Nicolis and Nicolis 1984). One such measure is the dimensionality of attractors, that is, the number of parameters necessary to control the time evolution in phase space. Some observations of weather variables (Fraedrich 1987; Essex *et al.* 1987) suggest low dimensionality which appears to be fractal and qualitatively characterizes chaotic behaviour. Another measure is the rate of divergence of initially close pieces of trajectories, which is a quantitative measure of the degree of chaos of the system, or its predictability.

(ii) *Dimensionality*. Consider data points randomly distributed on a line, on a surface, in a volume. The relative number of pairs of points, which are up to a distance l apart, grows linearly, quadratically, cubically with increasing l , that is, proportional to l , l^2 , l^3 . This qualitative view can be generalized to deterministic systems whose dynamics can evolve on relatively low-dimensional attractors embedded in phase space of higher dimension. The attractor dimension D_2 may then be estimated analogously using the cumulative distance distribution (correlation integral):

$$C(l) \sim l^{D_2} \quad \text{for } l \rightarrow 0 \quad (2.5)$$

generalizing the Euclidean distance (2.2) according to the phase space dimension (see, for example, Eckmann and Ruelle 1985 and references therein). A substitute phase space may be used when analysing data (given, for example, by single- or two-variable time series). Independent pieces of data trajectories of sufficiently long duration embed the attractor in a substitute phase space spanned by the time-lagged coordinates provided by the data. Then $C_m(l) \sim l^{D_2}$ for $l \rightarrow 0$ and m sufficiently large (see Packard *et al.* 1980). Note that in this study we are spanning a substitute phase space using two independent time trajectories, $x(t)$ and $y(t)$, whereas the more common type of nonlinear analysis of climatological data is based on a single variable.

(iii) *Predictability (degree of chaos)*. The probability, or relative number of cyclone pairs remaining within a fixed distance l , decreases with increasing duration of their time trajectory. Thus the change from $(m-1)\tau$ to $m\tau$ in duration and, related to it, from C_m to C_{m+1} in probability, provides a measure of the mean escape rate (divergence) of close pairs of pieces of trajectories from a tube of width l :

$$K_2 = (1/\tau) \ln C_m(l)/C_{m+1}(l), \quad \text{for } l \rightarrow 0, \quad m \rightarrow \infty. \quad (2.6)$$

Strictly speaking, K_2 is the order-2 entropy and provides a lower bound for the Kolmogoroff entropy, $K = \Sigma \lambda_i$. For smooth dynamics, K can be shown to be identical to the sum of all positive characteristic exponents $\lambda_i > 0$, corresponding to the expanding axes of an infinitesimally small error volume on the attractor. That is, $K > K_2 = -\lim(l/m\tau) \Sigma p^2(i_0, \dots, i_{m-1})$ for $m \rightarrow \infty$ and $\tau \rightarrow 0$; $p(i_0, \dots, i_{m-1})$ is the joint probability that the trajectory is in box i_0 at $t=0$, i_1 at $t=\tau$, ...; the sum is the probability that a pair of pieces of time trajectories fall into the same sequence of boxes (i_0, \dots, i_{m-1}) of the space-time partitioning (l, τ) with $(l, \tau) \rightarrow 0$ (see for example Eckmann and Ruelle 1985; Schuster 1984; and for a qualitative interpretation see Fraedrich

1987). The inverse value $1/K_2$ in the domain of constant D_2 -slopes defines a mean time scale (averaged over the attractor) up to which deterministic predictability may be possible, considering an e-folding rate of the divergence of initially close trajectory pieces.

The combination of (2.5) and (2.6) shows that the correlation integral $C_m(l)$ scales for $m \rightarrow \infty$ and $l \rightarrow 0$ as

$$C_m(l) \sim l^{D_2} \exp(-m\tau K_2).$$

Estimates of the cumulative distribution $C_m(l)$ are presented in a $\ln C_m(l)$ versus $\ln l$ diagram for increasing embedding dimension m , that is for pieces of cyclone tracks of duration $m\tau$. From these diagrams one can now derive, at least in principle, the saturation dimension of the attractor, D_2 , from the slopes of the $\ln C(l)$ graphs, which remain unchanged for sufficiently large embedding m , and the predictability, K_2 , from the distance between them.

(b) *A first application: Random walk cyclones with mean drift*

As a first application and to demonstrate the method we consider random walk (or Brownian motion) trajectories commencing from a regional pool of cyclones, whose initial positions $[x(t_i), y(t_i)]$ are given by a bivariate circular Gaussian distribution with mean $[\langle x(t_i) \rangle, \langle y(t_i) \rangle]$ and variance $s_x^2 = s_y^2 = s^2$. Furthermore, let the new locus of the cyclone after time step τ be independent of the previous one (except for a mean drift u, v) and generated by isotropic and Gaussian-distributed white noise g (with zero mean and the same variance s_g^2 for the x and y coordinates). Then the x position of the cyclone at time $t_i + k\tau$

$$x(t_i + k\tau) = x(t_i) + uk\tau + \sum_k g(k\tau) \quad (2.7)$$

is Gaussian distributed with mean $\langle x(t_i) \rangle + uk\tau$ and variance $s^2 + ks_g^2$; s^2 is the variance of the initial positions $x(t_i)$ and s_g^2 is the variance of the random noise g which is added after each time step τ . Furthermore, the x difference between the positions of two statistically independent cyclone events

$$d_x(k) = x(t_i + k\tau) - x(t_j + k\tau) = x(t_i) - x(t_j) + \sum_k g_i(k\tau) - \sum_k g_j(k\tau) \quad (2.8)$$

is also Gaussian distributed with zero mean and variance

$$S^2(k) = 2(s^2 + ks_g^2). \quad (2.9)$$

(i) *Correlation integral.* Identical expressions hold for the y difference due to the circular distribution of the initial positions and the isotropy of the random noise. Then, each of the two squared x - or y -difference components, $d_x^2(k)$ or $d_y^2(k)$, which enter the Euclidean distance (2.2), is chi-squared distributed. That is, the distribution of either one of the two components defining the squared distance $d_{ij}^2(k) = d_x^2(k) + d_y^2(k)$ has the gamma density (Feller 1966):

$$f_k(a; v) = (1/\Gamma(v)) a^v \{d_x^2(k)\}^{v-1} \exp\{-ad_x^2(k)\} \quad (2.10)$$

where $\Gamma(v)$ is the gamma function, $a = 1/2S^2(k)$, $v = 1/2 > 0$ or $n = 2v$ degrees of freedom; the expectation and variance of this distribution are v/a and v/a^2 , respectively. As the family of gamma densities is closed under convolutions (*), the sum of the two independent gamma-distributed variables of the same variance, $d_x^2(k) + d_y^2(k)$, remains gamma distributed, $f(a; v_1) * f(a; v_2) = f(a; v_1 + v_2)$, with $v_1 = v_2 = \frac{1}{2}$. Thus $d_{ij}^2(k) = d_x^2(k) + d_y^2(k)$ is gamma distributed with the exponential density f_k and the

related distribution function F_k :

$$\left. \begin{aligned} f_k &= \{1/2S^2(k)\} \exp\{-d_{ij}^2/2S^2(k)\} \\ \text{prob}\{d_{ij}^2(k) < l^2\} &= F_k = 1 - \exp\{-l^2/2S^2(k)\}. \end{aligned} \right\} \quad (2.11)$$

Since the $d_{ij}^2(k)$ are statistically independent on random walk cyclone tracks ($i = j$), (2.11) leads to the joint probability function of independent events (that is, of the squared distances $d_{ij}^2(k)$):

$$\text{prob}\{d_{ij}^2(k) < l^2 \text{ for } k = 0, 1, \dots, m-1\} = C_m(l) = F_0 F_1 \dots F_{m-1}. \quad (2.12)$$

From the distribution function $C_m(l)$ the dimensionality and predictability of the stochastic system can be deduced, which may then serve as a standard of comparison for the results obtained from data analysis.

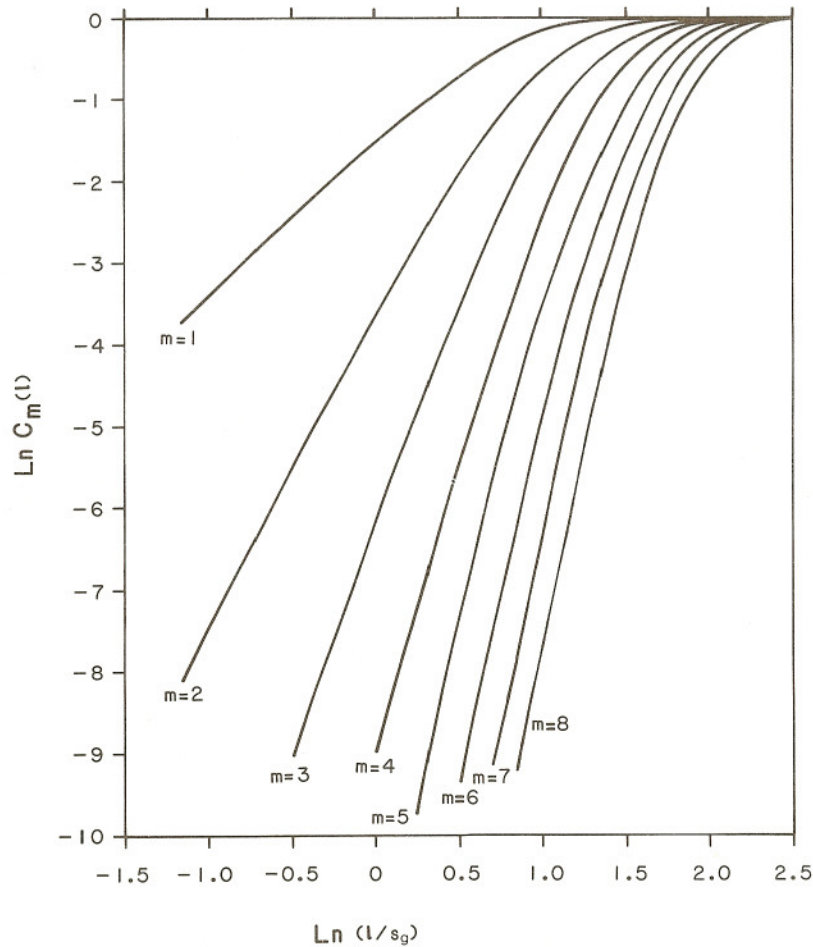


Figure 2. Random walk cyclones with mean drift: Theoretical cumulative distribution function $C_m(l)$ of the number of pairs of independent cyclone tracks remaining within the distance l for $m = 1, \dots, 8$ successive time steps. The $C_m(l)$ graphs are displayed in a $\ln C_m(l)$ versus $\ln(l/s_g)$ diagram with m increasing from left to right. Changes in the Gaussian white noise standard deviation, s_g , are additive. The slopes approach $D_2 \rightarrow 2m$ for decreasing distance threshold l , Eq. (2.13). Slope and distance lead to measures of dimension and entropy.

(ii) *Dimensionality*. The $C_m(l)$ graphs are displayed in a $\ln C_m(l)$ versus $\ln(l/s_g)$ diagram (Fig. 2). The distance l has been scaled by the Gaussian white noise standard deviation, s_g , and all cyclones are assumed to commence at the same location so that $s^2 = 0$ in (2.9). As expected from two-dimensional stochastic models, the slope D_2 of $\ln C_m(l)$ versus $\ln l$ for a given value of l increases in proportion to the duration as measured by m , and that

$$D_2 = d \ln C_m(l) / d \ln l = 2m \quad \text{for } l \rightarrow 0. \quad (2.13)$$

This result is obtained after introducing (2.12) into (2.13) and applying l'Hospital's rule. Thus the correlation dimension, D_2 , of a two-dimensional stochastic random walk process increases proportionally to each time step, and the constant of proportionality is given by the dimension of the state space of the stochastic system, that is, with each time step two new independent variables are created. This result can be generalized to deterministic processes, where the attractor dimension converges to a finite saturation value $D_2 \rightarrow D_\infty < 2m$, which may be fractal or non-integral.

(iii) *Predictability*. From empirically determined $C_m(l)$ graphs the mean rate of trajectory separation (or mean divergence) can be deduced. In the case of the stochastic cyclone model the definition (2.6) together with (2.12) leads to the following expression for the order-2 entropy:

$$K_2 = -(1/\tau) \ln F_m. \quad (2.14)$$

Here it becomes evident that K_2 is a measure (lower bound) of the Kolmogoroff entropy (or the degree of chaos), that is, the rate at which information about the state of an evolving system is lost. Thus, in the case of a stochastic system like the random walk cyclones, the degree of chaos or average rate of information loss (here K_2) tends to infinity both for $l \rightarrow 0$ (that is, with decreasing scale of the observational network measured in terms of cyclone distance l) and for $m \rightarrow \infty$ (that is, for generating information with each time step by successively adding random noise at fixed network scaling).

In this sense the inverse value, $1/K_2$, provides a mean time scale of predictability. At the required limit ($l \rightarrow 0$) it is not surprising that the predictability time scale ($1/K_2$) of a Gaussian stochastic system vanishes, as $K_2 = \infty$, after substituting (2.11) and (2.12) into (2.14). The same holds at a fixed distance threshold l , when lead times become larger ($m \rightarrow \infty$), that is, when more degrees of freedom (random noise) are added. Figure 3 shows this structure for random walk (cyclone) trajectories commencing at a fixed location (that is, $s^2 = 0$ in (2.9)). As in Fig. 2 the distance thresholds l are normalized by the Gaussian white noise standard deviation s_g .

3. RESULTS

The methods described in section 2 were applied to the three main Australian tropical cyclone regions shown in Fig. 1, individually and collectively. The numbers of tropical cyclones in these regions were 103, 47 and 99 respectively, a total of 249 tropical cyclones for the period 1959–1980. A tropical cyclone is designated as being in a given region if its initial position is in that region. Tropical cyclones may therefore, on occasion, move from one region to another or re-develop in another region during their life time.

(a) *Estimates of predictability time scales*

The basic approach adopted here is to calculate the correlation integrals given by Eq. (2.4). From the correlation integral the dimensionality and predictability can be deduced. It is noted that the distance norm corresponding to Eq. (2.2) is now the great

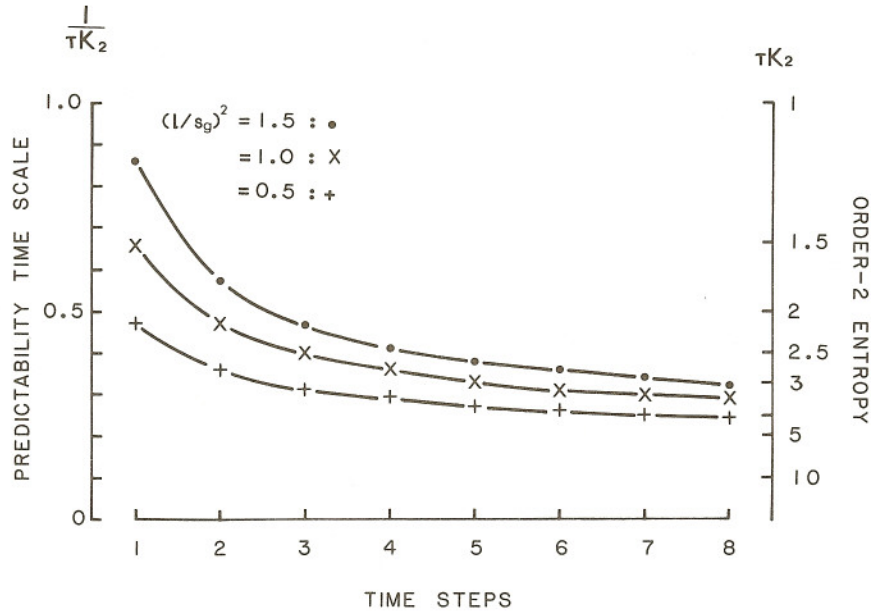


Figure 3. Random walk cyclones with mean drift: Predictability time scale (and order-2 entropy) depending on the duration m of the trajectory and the distance scale l which is normalized with the Gaussian white noise standard deviation, s_g .

circle distance, rather than the straight line distance. It is also noted that the calculations were performed twice, once with the original tropical cyclone position and once with the position normalized initially to a common origin. In the following we will discuss mainly the normalized results because the differences were negligible.

The analyses are displayed in a double logarithmic diagram (Figs. 4(a, b), with $\ln C_m(l)$ versus $\ln l$) to make direct estimates of the dimensionality of the processes involved and their predictability time scales as outlined in section 2. The following results should be mentioned:

(i) A chi-squared goodness-of-fit test was applied to compare the correlation integrals of the random walk or Brownian motion cyclone model (with mean drift, (2.12)) and the related empirical results, (2.4); that is, a theoretical and an empirical distribution are compared. The stochastic model has been calibrated by the observed position variances $S^2(k) = ks_g^2$, which increased linearly with the duration of the cyclone trajectory (2.9) and show best fit to the observations after $k\tau > 12$ hours (Fig. 5). This test leads to the rejection of the null hypothesis of the similarity between the distributions (on a 95% significance level).

(ii) The cumulative distribution functions (correlation integrals) of the observed cyclone tracks show a considerably smaller rate of increase in slope (dimension $D_2 < 2m$) with increasing lead time than that of the stochastic model. Note, however, that the empirical distributions do not exhibit an extensive linear domain (except for region 3 and perhaps region 1) which is consistent with that expected for asymptotic behaviour. Therefore we select $-8 < \ln C_m(l) < -4$ as a suitable interval where the counting frequencies are considered to be sufficiently large to allow meaningful estimates. A saturation dimension, $D_\infty = 6 - 7$, seems to be approached after $m = 15$ six-hour time steps. That is, no further increase in slope is expected when increasing the embedding dimension m . Not unexpectedly this is in agreement with results from analyses of mid-latitude weather.

suggesting it to be governed by a relatively low-dimensional attractor (Essex *et al.* 1987; Fraedrich 1987). Although saturation appears to have been reached, a small doubt remains because some subjective interpretation is involved in the limit process of fitting $C_m(l)$ to l^{D_2} for $l \rightarrow 0$.

(iii) Using the saturation dimension, estimates of the order-2 entropy K_2 , or predictability $1/K_2$, can be made, and provide a bound to the deterministic predictability in terms of an e-folding time scale for error growth. This predictability time scale is found to lie between 12 and 24 hours, estimated in the distance range $150 \text{ km} \leq l \leq 400 \text{ km}$.

Finally, some comments on the limitations of this method applied to cyclone tracks are in order. A cyclone track is an event of finite time span which does not necessarily cover the phase space completely. Thus, when constructing the substitute phase space using time-lagged coordinates, its dimension (necessary to embed the cyclone track attractor) is limited by the life time of the cyclones. Therefore, it is more appropriate to speak of average cyclone track predictability based on Lagrangian analogues when analysing the distance statistics than of predictability averaged over the weather attractor.

(b) Comparison with random walk tropical cyclones

The results of section 3(a) suggest that tropical cyclones in the Australian region have an e-folding error growth time scale of $1/K_2 \approx$ one day. The question that arises immediately is how do tropical cyclones behave beyond this predictability limit, which is the limit beyond which deterministic models cannot be used with confidence as forecasting tools. As a first attempt to examine this aspect we decided to see if the simple stochastic random walk model described in section 2(b) provides any insights. One of the results of this model is that the variance of positions grows linearly with time.

The observed variance of tropical cyclone position with time was plotted for each of the regions 1 to 3 and for the total region. These are given in Fig. 5 together with a random walk model commencing at 12 hours. It is clear immediately that there is a very close correspondence between the observed tropical cyclone and random walk cyclone variance between 18 and 60 hours. This close match between observed and random walk tropical cyclones gives further support for the deterministic predictability time scale of 12 to 24 hours.

Finally, some support for the relevance of a characteristic predictability time scale of about 18 hours is provided by the duration of straight line segments (to the nearest three hours). They are obtained from the Australian basin tropical cyclone tracks for the five seasons 1961–63 and 1975–78 (Lajoie 1984). It appears (Fig. 6) that the numbers of straight line segments on a tropical cyclone track which last longer than 18 hours, are almost equally distributed. However, the statistics of straight line segments of shorter duration show a more complex behaviour.

4. DISCUSSION AND CONCLUSIONS

The implications of the results obtained in section 3 are that for Australian region tropical cyclones the e-folding error growth time scale appears to be quite short, about one day. This time scale is consistent with the acknowledged position of the Australian–south-west Pacific basin as the region of greatest tropical cyclone track forecast difficulty (see, for example, Pike and Neumann 1987). It is also not surprising, therefore, that forecasting the movement of tropical cyclones in the Australian region has so far shown negligible skill.

It would appear, then, that for the Australian region, purely deterministic forecast

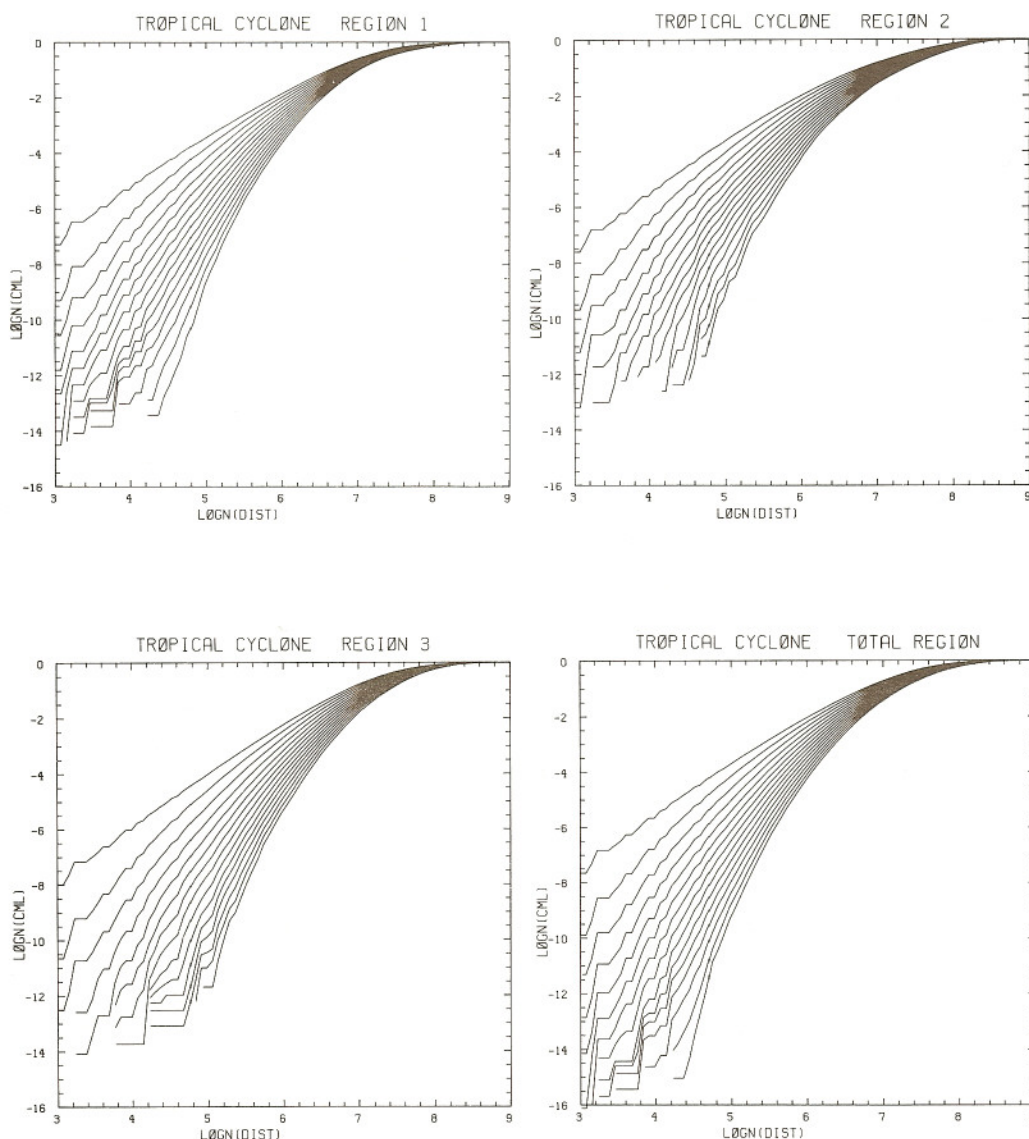


Figure 4(a). Cumulative distance distribution $C_m(l)$ of pairs of independent trajectory pieces displayed in a $\ln C_m(l)$ versus $\ln l$ diagram for a sequence of m six-hour time steps ($m = 1$ to 15). Tropical cyclone trajectories in the three geographical regions and the total Australian basin are analysed, with the position normalized initially to a common origin.

models cannot be expected to provide skilful forecasts much beyond the predictability time scale of about one day or so, because of the intrinsic sensitivity of the dynamics to the initial conditions.

A further interesting result discussed in section 3 was the close correspondence in the growth of tropical cyclone position variance, after about 18 hours, between the observed tropical cyclones and a theoretical model comprising a random walk process superimposed on a mean drift. This close correspondence after about 18 hours confirmed the anticipated role that stochastic models such as that of Keenan (1985)—in particular if they are based on climatological information including the mean drift—might be

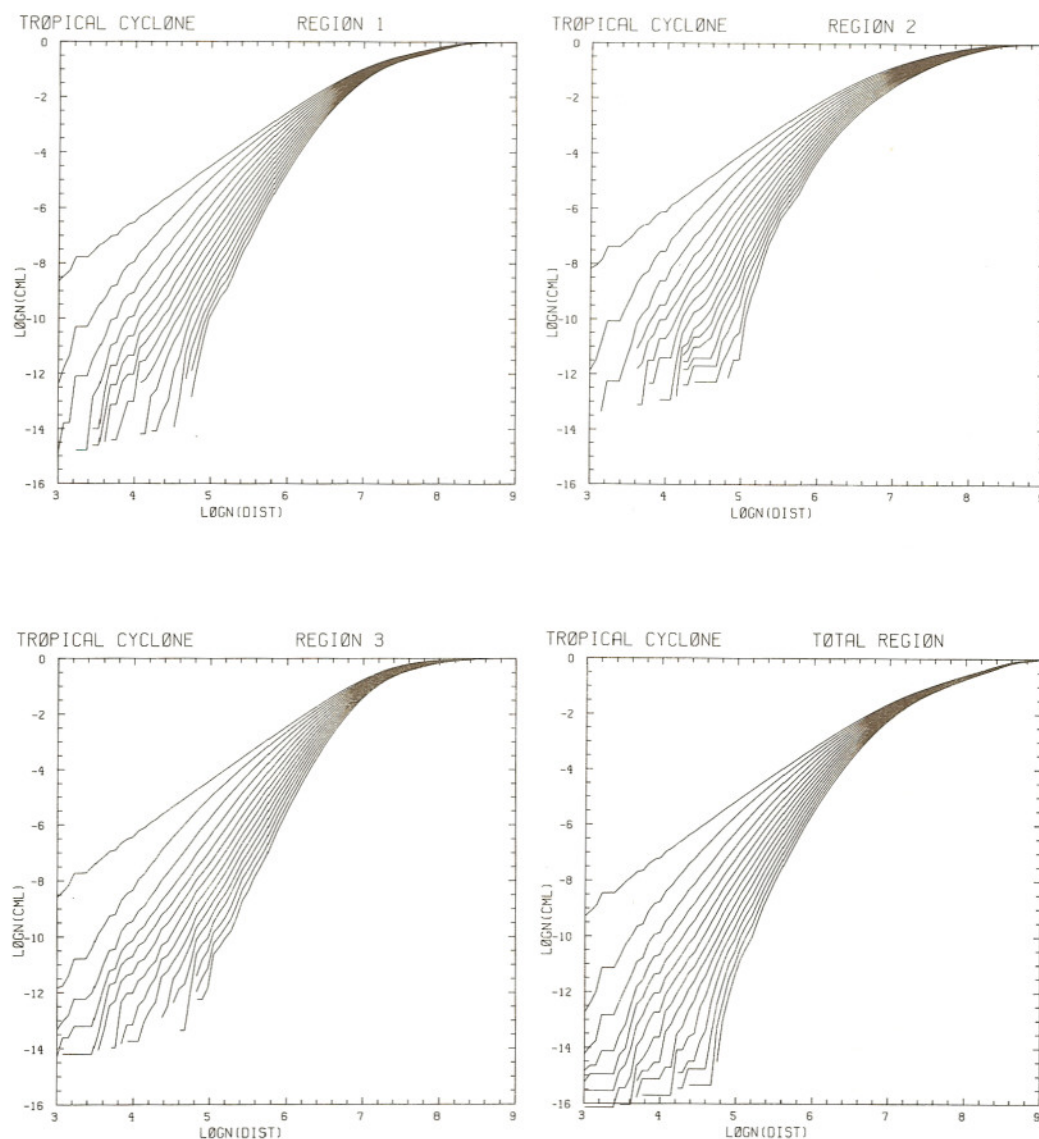


Figure 4(b). As (a) but with the position not normalized.

expected to play in forecasting tropical cyclone positions beyond the deterministic predictability time scale.

It should be noted that the techniques used in obtaining the e-folding error growth time scale are fairly new and are still being refined. In section 3, for example, it is mentioned that sometimes it is difficult to decide objectively whether the correlation integrals truly have reached saturation, particularly in cases where not all of the attractor has been captured. As yet the method used here may not allow for variable external forcing that might lead to a relatively large number of degrees of freedom in the deterministic processes.

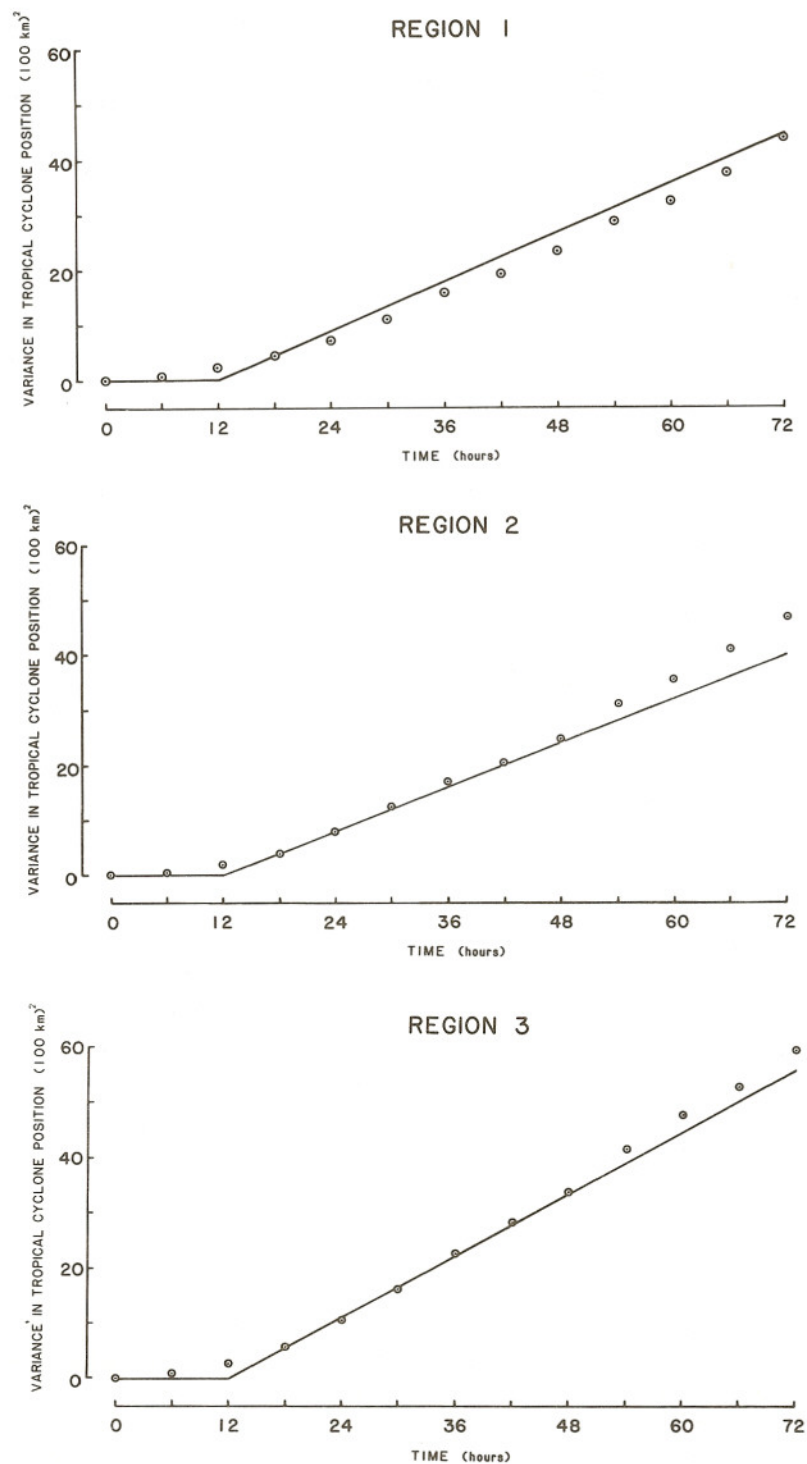


Figure 5. Variance of tropical cyclone positions in the Australian basin (regions 1 to 3 and the total region) changing with time. The observations (\odot) are compared with a mean drift random walk model (—) commencing after twelve hours mean drift.

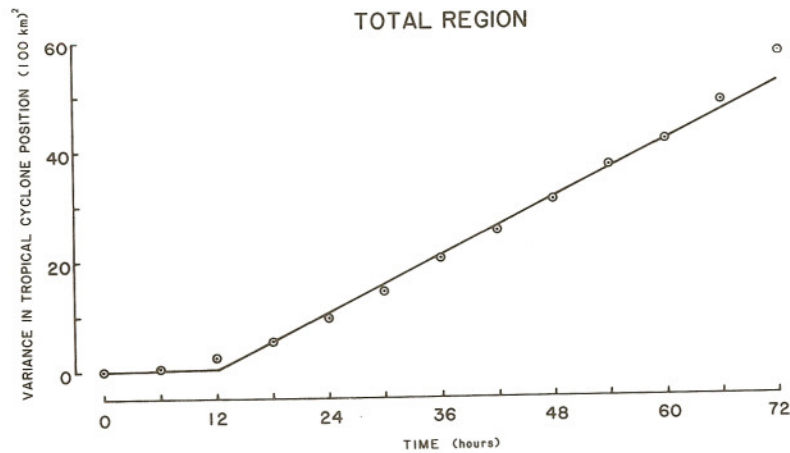


Figure 5 (continued).

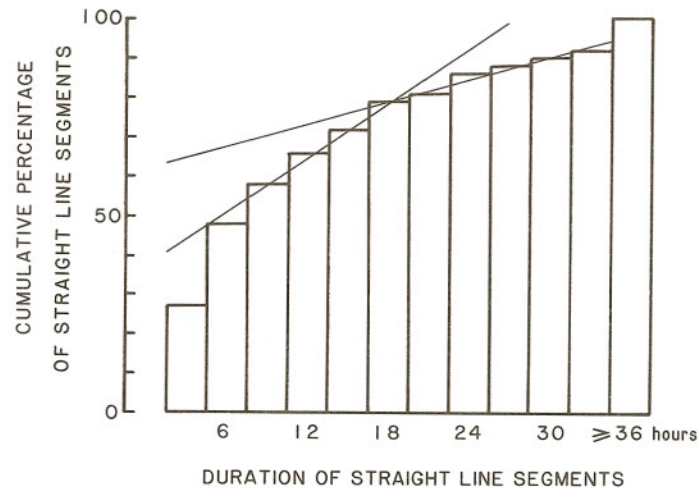


Figure 6. Statistics of straight line segments in the tracks of Australian basin tropical cyclones: Cumulative percentages of straight line segments versus their duration in three-hour intervals (after Lajoie 1984).

In a comparison study to be carried out in the future we intend to apply a similar methodology to that used in this study to examine the predictability characteristics of extratropical cyclone tracks. In the case of extratropical cyclone tracks, we expect that quite different dimensionality and predictability time scales will emerge.

ACKNOWLEDGMENTS

We would like to express our appreciation for the stimulating discussions on this topic we have had with BMRC staff, particularly Tom Keenan, Greg Holland and France Lajoie. We would also like to thank Kelvin Wong and Peter Yew for drafting assistance, Fay Stroumos and Lucie Crivera for typing the manuscript, and referees for their comments.

REFERENCES

- | | | |
|---|------|--|
| American Meteorological Society | 1979 | Policy statement of the American Meteorological Society on weather forecasting. <i>Bull. Am. Meteorol. Soc.</i> , 60 , 1453–1454 |
| Eckmann, J. P. and Ruelle, D. | 1985 | Ergodic theory of chaos and strange attractors. <i>Rev. Modern Phys.</i> , 57 , 617–656 |
| Essex, C., Lookman, T. and Nerenberg, M. A. H. | 1987 | The climate attractor over short timescales. <i>Nature</i> , 326 , 64–66 |
| Feller, W. | 1966 | <i>An introduction to probability theory and its applications</i> . Vol. II. John Wiley & Sons |
| Fraedrich, K. | 1987 | Estimating weather and climate predictability on attractors. <i>J. Atmos. Sci.</i> , 44 , 722–728 |
| Grassberger, P. and Proccacia, I. | 1984 | Dimensions and entropies of strange attractors from a fluctuating dynamics approach. <i>Physica</i> , 13D , 34–54 |
| Iwasaki, T., Nakano, H. and Sugi, M. | 1987 | The performance of a typhoon track prediction model with cumulus parameterization. <i>J. Meteorol. Soc. Jap.</i> , 65 , 555–570 |
| Keenan, T. D. | 1985 | Statistical forecasting of tropical cyclone movement in the Australian region. <i>Q. J. R. Meteorol. Soc.</i> , 111 , 603–615 |
| Lajoie, F. A. | 1984 | 'Report on the movement of tropical cyclones in the Australian region'. Australian Bureau of Meteorology, Technical report 58 |
| Lorenz, E. N. | 1985 | 'The growth of errors in prediction'. Pp. 243–265 in <i>Turbulence and predictability in geophysical fluid dynamics and climate dynamics</i> . Eds. M. Ghil, R. Benzi and G. Parisi. North-Holland |
| McBride, J. L. and Holland, G. J. | 1987 | Tropical cyclone forecasting: a worldwide summary of techniques of verification statistics. <i>Bull. Am. Meteorol. Soc.</i> , 68 , 1230–1238 |
| Neumann, C. J. and Pelissier, J. M. | 1981 | Models of the prediction of tropical cyclone motion over the North Atlantic: An operational evaluation. <i>Mon. Weather Rev.</i> , 109 , 522–538 |
| Nicolis, C. and Nicolis, G. | 1984 | Is there a climate attractor? <i>Nature</i> , 311 , 529–532 |
| Packard, N. J., Crutchfield, J. P., Farmer, J. D. and Shaw, R. S. | 1980 | Geometry from a time series. <i>Phys. Rev. Lett.</i> , 45 , 712–716 |
| Pike, A. C. and Neumann, C. J. | 1987 | The variation of track forecast difficulty among tropical cyclone basins. <i>Weather and Forecasting</i> , 2 , 237–241 |
| Schuster, J. G. | 1984 | <i>Deterministic chaos</i> . Physik Verlag, Weinheim |